INFORMATICS JOURNALS
The Journal of Electrochemical Society of India, Volume 74, Issue (7&8), October – December 2025; pp. 176–184
ISSN (Print) : 0013-466X
ISSN (Online) : xxxx-xxxx
DOI: 10.18311/JESCI/2025/54170

All Soluble Redox Flow Batteries beyond Vanadium: A Future Perspective

Moothedath Aparnasree[1,2] and Mani Ulaganathan[2,3]*

[1]*Department of Chemistry, Amrita School of Physical Sciences Coimbatore, Amrita Vishwa Vidyapeetham, Coimbatore – 641112, Tamil Nadu, India*
[2]*Functional Materials Laboratory, Amrita School of Engineering Coimbatore, Amrita Vishwa Vidyapeetham, Coimbatore – 641112, Tamil Nadu, India*
[3]*Department of Physics, Amrita School of Physical Sciences Coimbatore, Amrita Vishwa Vidyapeetham, Coimbatore – 641112, Tamil Nadu, India*

Abstract

Redox Flow Batteries (RFBs) have emerged as one of the most promising solutions for large-scale, long-duration energy storage. RFBs store energy in external reservoirs containing soluble, redox-active species, allowing the decoupling of energy and power, which can be scaled independently by adjusting the electrolyte volume and cell size. The commonly used redox flow battery is an all-vanadium system, where the electrolyte exists in multiple oxidation states, which helps reduce cross-contamination during operation; however, the low energy density and high cost of the VRFB electrolyte material hinder its widespread application. In this review, alternative all-soluble redox flow battery systems, such as those based on all-iron, all-chromium, iron-chromium, polysulfide-iodine, and polysulfide-bromine, are discussed.

Keywords: All-soluble RFB, Halide-based RFB, Low-cost, Recyclable, High-energy density

1. Introduction

To tackle the ever-increasing energy demand, various types of energy storage systems are available, including pumped hydro storage, flywheels, compressed air, and electrochemical energy storage devices[1-7]. Among them, electrochemical energy storage systems, specifically batteries, have attracted significant attention due to their features, including a flexible design, greater durability, and a wide range of applications, from small gadgets to large-scale and off-grid grids[8]. In this regard, the redox flow battery is one of the most prominent energy storage devices for high-energy and long-term applications, as its energy is stored in an external reservoir of charged redox species[9]. Due to the decoupled nature of this system, the energy and power density of this battery can be independently upgraded by increasing the electrolyte molarity or volume, and to increase the power density, the battery area can be varied[10]. The first-generation redox flow battery is the iron-chromium, developed by NASA in 1970; it uses Fe^{2+}/Fe^{3+} and Cr^{3+}/Cr^{2+} electrolytes in the positive and negative compartments, respectively, delivering a maximum cell voltage of 1.18 V vs. SHE. Even the poor kinetics of the Cr^{3+}/Cr^{2+} redox couple, as well as membrane crossover, limit its wide-range application[11]. To overcome the limitations of the Fe-Cr RFBs, Maria *et al.*[12] invented and successfully demonstrated the all-Vanadium Redox Flow Battery (VRFB), where vanadium dissolved in sulfuric acid has been used as both anolyte and catholyte; the combination of the V^{4+}/V^{5+} (1 V vs. SHE) and V^{2+}/V^{3+} (-0.26 V vs. SHE), showing the total cell voltage of 1.26 V vs. SHE. To date, this is the most commonly used redox flow battery in large or grid-scale applications due to its advantage in the same type of electrolyte ions in both compartments, so it limits the cross-contamination, longer life cycle up to 10,000

*Email: m_ulaganathan@cb.amrita.edu, nathanphysics@gmail.com

cycles with a minimal capacity loss, depth of discharge, non-flammable electrolyte, and environmentally friendly, *etc.*[13]. Even though the wide range of use for this VRFB is limited by the high cost of vanadium metal, its limited energy density (around 20-35 Wh L^{-1}), temperature sensitivity, and membrane degradation, among other factors[14]. Therefore, it is crucial to identify alternative redox chemistries for a more effective replacement for the VRFB. The Zn-based RFB has attracted attention for its high energy density and low cost. Like all vanadium RFBs, the Zinc-Bromine RFB has been commercialised. However, dendrite formation due to Zn/Zn^{2+}, poor cycle life, and other limitations limit its development as much as those of all vanadium RFBs[15]. The one that can be developed to replace all vanadium is the other all-soluble RFB, in which both the redox species in the catholyte and anolyte are soluble, and no deposition or dissolution reactions occur. In this context, all soluble-redox flow batteries beyond vanadium are widely investigated, such as those based on Iron, chromium, iron-chromium, and halide systems[16,17]. All iron RFBs have attracted research attention due to their advantages in material abundance, low cost, and good reversibility. At the same time, the iron-chromium RFB offers reduced cross-contamination, lower operating costs, and a long-life cycle[18,19]. The halide redox flow battery uses the redox couples of (Cl^-/Cl_2, Br^-/Br_2 or I^-/I_2)[20]. These are highly soluble redox-active species with excellent reversibility; the halide-based redox kinetics are high-speed in electron transfer, reducing crossover, and good reversibility. This review systematically discusses the recent advancements in the aforementioned redox flow batteries, including those with Iron-Chromium (Fe-Cr), all chromium (all-Cr), all iron, polysulfide-halide RFBs.

To mitigate the issues faced by the all-soluble vanadium RFB, other all-soluble RFBs have to gain attention for large-scale applications. All soluble Redox Flow Batteries (RFBs) can be classified into two primary types based on the redox-active species employed: metal-based and halide-based systems[21]. Scheme 1 provides an overview of all soluble redox flow batteries. In metal-based redox flow batteries, transition-metal redox species are used, with the resulting products being soluble in both the catholyte and anolyte, thereby preventing metal deposition. Examples of such transition metals include chromium and iron[22]. Conversely, halide-based RFBs employ halides, such as chlorine, iodide, and bromide, as anolytes, while utilising non-metallic redox species as catholytes, such as polysulfide iodide and polysulfide bromine[17]. This review offers a concise perspective on the future of soluble redox flow batteries.



Scheme 1. Overview of all-soluble redox flow battery.

2. All Soluble Metal-based Redox Flow Batteries

All-soluble RFB has gained research interest in recent times due to its advantage of soluble redox species in the electrolyte; the redox species can be the same type of ionic species or different types[16]. The most commonly used all-soluble electrolyte is vanadium in the form of V^{4+}/V^{5+} and VO^{2+}/VO_2^+. There are no solid-phase redox reactions, unlike in hybrid RFBs[23]. Since the energy and power density of the RFBs are highly dependent on the concentration of the redox species, a wide variety of organic and inorganic additives have been tailored to enhance performance, and this process can also be easily scaled up. However, the primary concern about VRFBs is the high cost of vanadium and their limited energy density, which makes it crucial to replace them with other cell chemistries[23,24]. In this regard, the different types of all-soluble redox flow batteries have been investigated, including all-chromium[25], iron-chromium[26], and all-iron[27], as well as all VRFBs. The initial concept of the redox flow battery (RFB) was patented by Kangro in 1947, and NASA further refined this during the development of Iron-Chromium (Fe-Cr) RFBs[25]. The poor conductivity of Cr^{3+}, low columbic efficiency (CE), hydrogen evolution at the anode, and electrolyte crossover in the first created Iron-Chromium RFBs (ICRFBd) limited

their commercialization[26]. To find a solution for this, Li *et al.*[28] constructed an Fe-Cr (Iron-Chromium) RFB with a complex electrolyte of Cr-ethylenediaminetetraacetic acid chelate (Cr-EDTA)/2-methylimidazole(2-MI) as an anolyte and Potassium ferrocyanide (K_4FeCN_6) electrolyte as catholyte. The 2-MI helped replace the H_2O ligand in the Cr-EDTA and serves as an electron-transfer channel. The new electrolyte combination helps suppress HER and increase conductivity. The RFB achieves coulombic and energy efficiencies of 97% and 76%, respectively, even after 80 cycles with an OCV of 1.6 V due to the complexing electrolyte combination. The general cell reactions of ICRFBs are given in equations[26] (1-3)

$$Fe^{2+} \leftrightarrow Fe^{3+} + e^{-} \quad E^0 = 0.77 \ V \ vs. \ SHE \tag{1}$$

$$Cr^{3+} + e^{-} \leftrightarrow Cr^{2+} \quad E^0 = -0.41 \ V \ vs. \ SHE \tag{2}$$

$$Cr^{3+} + Fe^{2+} \leftrightarrow Cr^{2+} + Fe^{3+} \quad E^0 = 1.18 \ \ V \ vs. \ SHE \tag{3}$$

Later, all-chromium redox flow batteries have gained attention due to the three soluble oxidation states of chromium[29]. In the past, HCl was used as an electrolyte for chromium, which is corrosive and has a short life cycle. Pecsok *et al.*[30] and Walsh *et al.*[31] have reported that the ETDA complex can increase the Cr(II)/Cr(III) reactions. Inspired by this, Bae *et al.*[32] investigated the all-chromium RFB with the Chromic potassium sulphate [$KCr(SO_4)_2$], Ethylenediamine-Tetra Acetic Acid (EDTA) complex electrolytes. The flow cell delivers the current efficiency of 99% with the power output of 0.37 W at 30 mA cm^{-2} at the electrolyte concentration of 0.2 M Cr (III) EDTA electrolyte. The energy efficiency is limited by the sluggish kinetics of the chromium complexes, which show further development of all chromium RFbs.

The other all-soluble metal-based RFB is the all-iron RFB (AIRFB), which is of two types: one with dissolution/deposition and the other an all-soluble system[33]. L.W. Hruska and R. Savinell formulated the existing all-Iron RFB in the early 1980s. In that the system is constructed by the Fe2+/Fe0 and Fe2+/Fe3+ redox pairs. Robert Savinel et al.,[34] demonstrated the operation of AIRFB and showed that increasing the chlorine anion concentration in the anolyte reduces hydrogen evolution and increases the coulombic efficiency of iron plating[35,36]. Whereas Gong *et al.*[27] investigated All-Iron Redox Flow Batteries (AIRFB) using the Iron-Triethanolamine (Fe-TEOA) and iron cyanide (Fe-CN) redox couples, which provide all soluble redox couples.

Figure 1 shows the redox reactions of various all soluble redox flow batteries reported in the literature. [Fe(TEOA)OH]$^{-}$/[Fe(TEOA)(OH)]$^{2-}$) and an iron–cyanide redox pair (i.e., $Fe(CN)_6^{3-}/Fe(CN)_6^{4-}$) delivers the maximum cell voltage of 1.34 V vs. SHE are given in equation 4-6. The anolyte contains 0.2 M $FeCl_2$, 1 M TEOA, and 1.5 M NaOH, whereas the catholyte contains 0.2 M $Na_4Fe(CN)_6$ in 2 M NaOH, respectively. The reaction mechanism associated with the Iron-Cyanide redox flow system is given:

$$\left[Fe(TEOA)OH\right]^{-} + e^{-} \leftrightarrow \left[Fe(TEOA)(OH)\right]^{2-} \quad E^0 = -0.86 \ V \ vs \ SHE \tag{4}$$

The posolyte has prominent redox peaks at the anodic and cathodic side with the conversion of $Fe(CN)_6^{3-}$ to $Fe(CN)_6^{4-}$ at the standard reduction potential of 0.48 V vs. SHE. The half and overall cell reactions of all Iron-RFB are given:

$$Fe(CN)_6^{3-} + e^{-} \leftrightarrow Fe(CN)_6^{4-} \quad E^0 = 0.48 \ V \ vs \ SHE \tag{5}$$

Overall, Cell reaction:

$$\left[Fe(TEOA)(OH)\right]^{2-} + Fe(CN)_6^{3-} \leftrightarrow \left[Fe(TEOA)OH\right]^{-} + Fe(CN)_6^{4-} \quad E^0 = 1.34 \ V \ vs \ SHE \tag{6}$$

The CV curve exhibits a peak-to-peak separation of 61 mV, indicating highly reversible reactions. On the other hand, the negolyte also shows a prominent peak at both the anodic and cathodic sides, corresponding to the conversion of $[Fe(TEOA)OH]^{2-}$ to $[Fe(TEOA)OH]^{-}$, with a very minimal peak-to-peak separation of 64 mV. The constructed all-iron RFB with the electrolyte as mentioned earlier delivers coulombic, voltage, and energy efficiencies of 93%, 78%, and 73%, respectively, at a current density of 40 mA cm^{-2} with a flow rate of 100 $Lmin^{-1}$ by using Nafion 212 membrane the polarization curve at various current densities from 0-400 mA cm^{-2}, it delivers the maximum power density of 160 mW cm^{-2}. Similarly, Yu *et al.*[37] constructed a redox flow battery thaconsists of a ferrous sulphate ($FeSO_4$) electrolyte, along with the supporting electrolyte of 1-ethyl-3-methylimidazolium chloride (EMIC), on both sides of the flow cell. The Fe^{2+}/Fe^{3+} electrolyte reaction of Fe^{2+}/Fe^{3+} takes place on the positive side, and on the negative side, the Fe^0/Fe^{2+} reaction takes place. They constructed an all-iron redox flow cell with a flow rate of 60 L min^{-1}. The $FeSO_4$/EMIC||micro porous membrane||$FeSO_4$/EMIC cell is tested up to 800 cycles by applying the regeneration technique after every 50

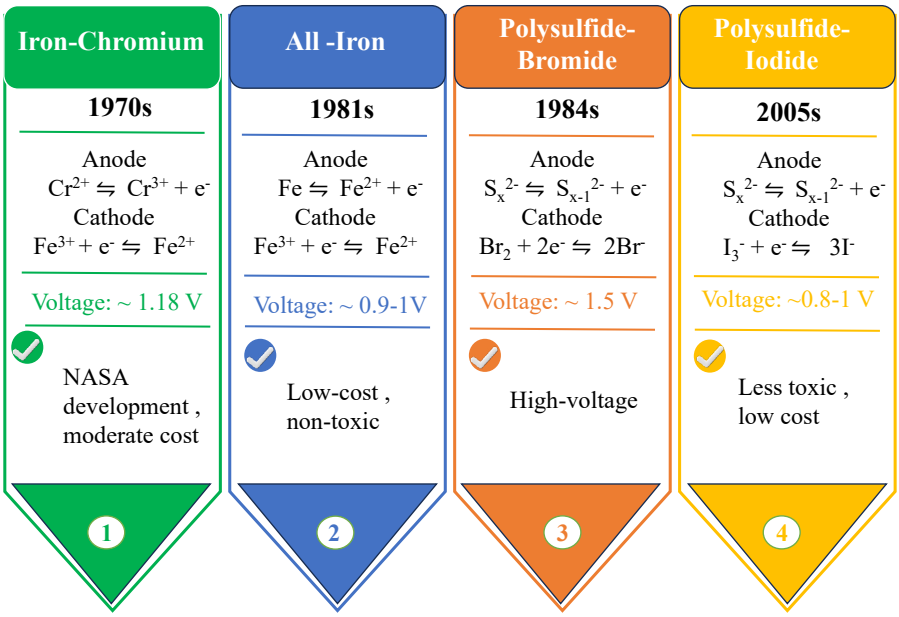


Figure 1. Redox reactions of various all-soluble redox flow batteries reported in the literature.

cycles with 2 M $FeSO_4$ and 0.1 M EMIC electrolyte at a current density of 20 mA cm^{-2}. The coulombic efficiency initially showed 70%, decreasing to ~65% after cycling. The EMIC improves the uniformity of iron deposition on the electrode. Modifying the electrolytes, membrane, and electrodes will further enhance the performance of metal-based all-soluble RFBs.

3. All Soluble Halide-based Redox Flow Batteries

As discussed in the previous section, halide-based batteries can be utilised for large-scale applications because the redox species present in both the catholyte and anolyte are soluble and can be reused. In a halide-based RFB, sulfur, which is considered the 14th most abundant element in the Earth's crust, and low-cost is used as the anolyte medium[38]. It is known to exist as a polysulfide, which offers several advantages, including a multielectron redox reaction and a high theoretical energy density of ~160 Wh L^{-1}. Aqueous polysulfide-based redox flow batteries are favourable for large-scale energy storage applications due to their high solubility of ~ 8.8 mol L^{-1} in H_2O and low cost[39]. These polysulfide electrolytes have been extensively studied as high-capacity, low-cost electrolytes for RFB due to their advantages. When these are combined with the halides like iodine and omine species, a suitable energy storage RB can be developed, known as polysulphide bromide (S_x^{2-} / Br_2) and polysulfide iodide (S_x^{2-} / I^-). During charging, the long chain polysulfide (S_4^{2-}) gets reduced to form short chain polysulfide or sulfide ions(S^{2-}) with the cleavage of the disulfide bonds(-S-S-). During discharge, the process reverses (equation 7)[40]. Although polysulfide-based RFB has merits, it faces several significant challenges, including poor kinetics, low energy efficiency, and a limited lifespan[41]. Schematic representation of the all-soluble S-I^2 rodox flow cell is shown in figure 2.

Polysulfide Bromine Redox Flow Battery (PBRFB) was reported in the early 1980s by Remick (R.J. Remick, P.G. Ang, U.S. Patent) and subsequently by Regenesys Ltd.[42]. Sodium polysulfide/bromine was primarily developed by the UK company Innogy, where aqueous sodium polysulfide and bromide solution serves as the catholyte and anolyte. A Nafion membrane, which conducts Na^+, is used as a separator in these cells. This sodium ion passes through the membranes to maintain neutrality and to provide current flow[38]. However, the crossover of the electrolytes and self-discharge reduced their cycle life by 50-60, thereby hindering their commercialisation. The solubility of the electrolytes is significant in redox flow batteries, as it helps increase energy density. Ahmad *et al.*[43] formulated a novel anolyte for the PBRFB system to increase the solubility of sulfur in the polysulfide electrolyte, thereby improving the charge density by using elemental sulfur and sodium polysulfide. Different concentrations of elemental sulfur have been added to the sodium sulfide nano-hydrate

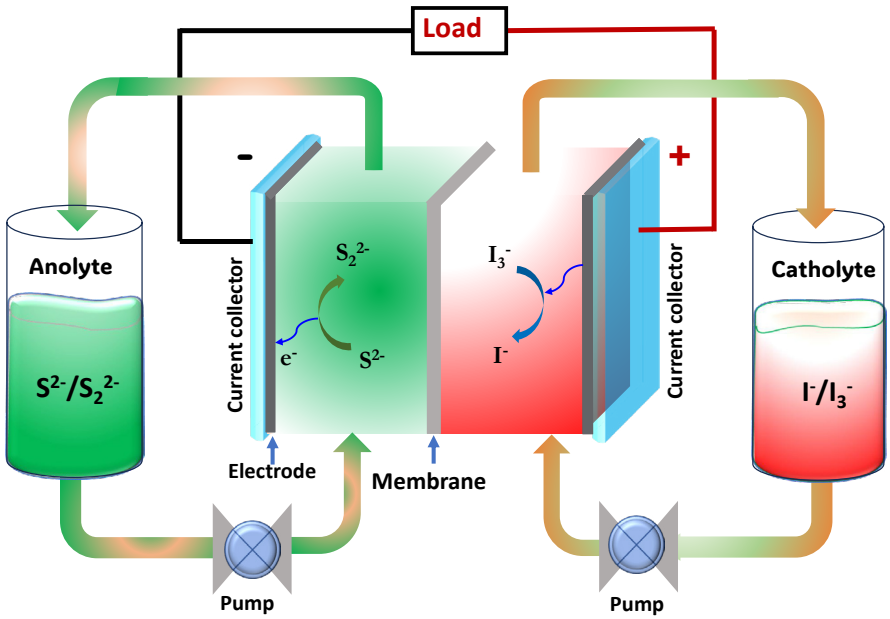


Figure 2. Schematic representation of the S-I2 all-soluble redox flow cell.

($Na_2S.9H_2O$) solution with a ratio S/Na of 0.5 to 2.4; that 1:4 ratio is the optimised ratio[44,45]. Various molar ratios of the Elemental Added Sulfur Sodium Polysulfide (EASSP) anolyte and NaBr catholyte were studied, and 1.4 M (EASSP) and 8 M NaBr were the optimised concentrations. The cycling stability of the system is determined using 1.4 M EASSP and 8 M NaBr at a flow rate of 30 mL/min. The cell delivers a capacity of ~17 mAh and a columbic efficiency of ~98% over 150 cycles, with no degradation. The addition of elemental sulfur reduced the sulfur passivation layer at the electrode and increased the density. The overpotential decreases as the NaBr concentration increases to 8 M, due to the excess of Br_3^-. The half-cell analysis of the catholyte (equation 8) and the anolyte (equation 7) of the PBRFB undergoes the basic reaction and achieves a theoretical cell potential of 1.55V.

$$2S_2^{2-} \leftrightarrow S_4^{2-} + 2e^- \quad E^0 = -0.51\ V\ vs\ SHE \tag{7}$$

$$Br_3^- + 2e^- \leftrightarrow 3Br^- \quad E^0 = 1.05\ V\ vs\ SHE \tag{8}$$

Gross *et al.*[46] in their work, they reported that an increase in the overpotential of the flow cell at the time of cycling will cause an increase in the mass transport resistance, which simultaneously decreases the Br_3^- concentration, and the Br^-/Br_2 cell reaction takes place (equation 9).

$$2Br^- \leftrightarrow Br_2 + 2e^- \tag{9}$$

Zhou *et al.*[47] reported that slight variations in the electrochemical activity of the electrode determined the cell voltage. They found that Carbon Felt (CF) and Activated Carbon (AC) 3D electrodes performed similarly, but AC's mass transport limitations hindered its efficiency. CF coated with a catalyst achieved over 80% energy efficiency after 50 cycles, while AC reached only 64.7% after 15 cycles, highlighting CF's superior performance for PSB flow batteries and reduced sulfur passivation. Zhao *et al.*[48] reported that using Ni/C as the positive electrode and Pt/C as the negative electrode will increase the power density as well as the efficiency of polysulfide/bromide RFB. The importance of 3D printed electrodes in PSR batteries is well explained by Yeetsorn *et al.*[49].

Ion crossover is a key challenge in such PBRFB systems, leading to sulfide precipitation and its accumulation on the electrode. Additionally, the formation of volatile and toxic Br_2 limits its large-scale production[51]. As a result, iodide is considered a better option, as it has faster reaction kinetics and a higher volumetric capacity. Due to the high solubility of the sulfide/polysulfide and iodide/triiodide redox couples, these were considered promising for a high-energy all-soluble redox flow battery[38]. Li *et al.*[40] used KI (Potassium Iodide) and K_2S_2 (Potassium Polysulfide) as catholyte and anolyte, respectively. The peak-to-peak separation of iodide is 101 mV, whereas for the sulfide it is around 381 mV. This indicates that iodide ions have better reaction kinetics than sulfide ions. To avoid ion crossover, Nafion-117 and

Nafion-115 membranes were used. The system delivers an overall cell voltage of 1.05 V. The half-cell reaction for the PSIRFB is shown in equations (7,10)

$$I_3^- + 2e^- \leftrightarrow 3I^- E^0 = 0.54\ V\ vs\ SHE \quad (10)$$

The system achieves a capacity retention of over 98% with a coulombic efficiency of 97% at the 50th cycle. This work reports the influence of flow rate and current density on the system's performance, and it also has a lower material cost than all vanadium RFBs. To further improve battery performance, Rahimi *et al.*.[50] used a magnetic nanofluidic electrolyte with magnetic carbon nanotubes on the catholyte side of the polysulfide RFB. By dispersing magnetic multiwalled carbon nanotubes (MMWCNTs), a highly stable magnetic nanofluidic electrolyte was prepared at a concentration below 0.3 g. As the concentration of MMWCNTs in the catholyte increases, the power density increases and the slope of the curve decreases, indicating a low specific area resistance (ASR). Thus, the magnetic electrolyte helps to increase the electrochemical performance similar to that of a catalyst. Wang *et al.*.[52] designed defective MoS_2 electrodes with a Co single-atom (CoSA) catalyst on the nanosheets to improve the sluggish redox kinetics of the PSIB. To suppress HER reaction and improve kinetics on the sulfide side, Huang *et al.*[53] employed the Kirkendall effect to design a Cu7S4 nanocage that increased the electrode's surface area. Rahimi *et al.*[54] proposed a Magnetic Flowable Electrode (MFE) to improve the system's performance. As with electrolytes, electrodes also play a significant role in RFBs, as discussed earlier. Thus, all soluble RFBs investigated so far will be equally potential candidates, given their merits. However, these systems must be thoroughly investigated to compete with the existing all-vanadium and Zn-Br_2 commercialised RFBs. The performance characteristics of various RFBs with all soluble redox-active elements are summarised in Table 1.

4. Outlook and Future Perspective

All Iron: Although the All-Iron Redox Flow Battery is widely investigated as a sustainable alternative for large-scale, long-duration energy storage, it is limited by the material's abundance and the non-toxic nature of iron-

Table 1. The comparison of flow cell performance of all iron, all chromium, iron chromium, polysulfide-bromine, and polysulfide-iodine

System	Catholyte	Anolyte	Electrode	Membrane	Cell potential	CE (%)	EE (%)	Current density	Cycle number	Power density	Flow rate	Reference
All Iron	0.2 M $Na_4Fe(CN)_6$ + 3 M NaOH	0.2 M $FeCl_2$ + 1 M TEOA + 1.5 M NaOH	Carbon paper	Nafion 212	1.34 V	93	73	40 mA cm^{-2}	110	160 mW/ cm^2	100 mL/ min	27
	0.5 M $Fe(CN)_6$	0.5 M Fe(DIPSO)	Carbon felt	Nafion-212	1.37	99.5	68.5	80 mA cm^{-2}	100	93.2 mW/ cm^2	23 mL/min	55
	2 M $FeSO_4$ + 0.1 M EMIC	2 M $FeSO_4$ + 0.1 M EMIC	Carbon felt	Microporous membrane	1.21	70	-	20 mA cm^{-2}	800	-	60 mL/min	37
All chromium	$KCr(SO_4)_2$EDTA+1 M sodium acetate	$KCr(SO_4)_2$ EDTA+1 M sodium acetata	graphite felt	Ion-exchange membrane	1.37 V	99	-	30 mA cm^{-2}	-	-	0.0047 mm S^{-1}	32
Iron-chromium	2 M K_4FeCN_6	Cr(EDTA) (2-MI)	Graphite felt	N212	1.6 V	97	76	50 mA cm^{-2}	80	-	-	28
	1 M $FeCl_2$ + 1 M $CrCl_3$+ 3MHCl+0.005 M Bi_2O_3	1 M $FeCl_2$ + 1 M $CrCl_3$+ 3MHCl+0.005 M Bi_2O_3	Graphite felt	Nafion-212	1.18 V		79.6	200 mA cm^{-2}	65	178 mW/ cm^2	50 mL/min	56
Polysulfide-bromine	4 M NaBr	1.3 M Na_2S_4	Co-GF, GF	Nafion-117	1.4 V	96.1	81.0	40 mA cm^{-2}	50	-	200 mL/ min	47
	8 M NaBr + 1.4 M EASSP	1.4 M$Na_2S{\cdot}9H_2O$	Graphitic felt	Nafion-1110,117	1.55 V	98	-	40 mA cm^{-2}	150	-	-	43
Polysulfide-iodine	4 M KI	3 M K_2S_2 + 1M KOH	Carbon felt	Nafion-115 ,117	-	93.06	73.01	15 mA cm^{-2}	50	-	4-10 mL/ min	40
	2.8 M KI+1 M KOH	3 M K_2S_2 + 1.5 M KCl + 0.3 g L^{-1}MMWCNTs	Carbon felt	N117	1.	~100	-	30 mA cm^{-2}	200	69 mW/ cm^2	40 mL/min	50

based aqueous electrolytes. However, the main challenges include instability of Fe^{2+}/Fe, precipitation, hydrogen evolution, and ion crossover. Also, recent advances in electrode engineering, electrolyte optimisation, and membrane optimisation are key research topics in the all-iron RFB system. In the future, the research will focus on dendrite growth suppression, electrolyte formulation, membrane engineering, and iron hydrolysis to achieve scalability, long cycle life, and reduced cost for AIFRBs, which will enable their commercialisation.

Iron-Chromium: Despite the many advantages of Cr-Fe RFBs, the system lags due to its low cell voltage of 1.18 V and low energy density. The factors include HER, electrolyte stabilisation, electrode surface modification, sluggish Cr^{3+}/Cr^{2+} kinetics, and capacity fading over cycling. Recent research advancements, such as electrolyte optimisation through the addition of buffer solutions, complexing agents, and mixed acid formulations, have increased interest in the Fr-Cr system. The future perspective focuses on improving cycle life (>10,000 cycles) and scaling cost-effective manufacturing to megawatt-hours for the Fe-Cr RFB system.

Polysulfide-Bromine: The Polysulfide-Bromine RFB has attracted attention as a next-generation energy storage system due to its low material cost, environmentally benign materials, and high theoretical energy density. The significant advantage of this system is its 1.5 V cell voltage, which is suitable for a stationary energy storage system. Although the cell voltage and energy density are higher than those of the VRFB, it still faces many issues, such as crossover, sluggish sulfide kinetics, Br_2 gas evolution, electrode corrosion, and capacity fading during long-term operation. These can be overcome by properly optimising the electrolyte on both sides, modifying the electrode used, and improving mass transport. The continued progress in these areas can lead to polysulfide-bromine as a better replacement for VRFB and Zn-based redox flow battery systems.

Polysulfide-Iodide: The polysulfide-iodide RFBS are an up-and-coming alternative to the all-vanadium redox flow battery due to their low cost, environmental friendliness, and earth-abundant active materials. But this system still lags due to the Sulfide ion's sluggish kinetics; ion crossover leads to capacity fade over cycling, resulting in a loss of energy density. Most cost-effective and environmentally friendly RFB, but it faces key challenges such as low energy and power density, poor electrochemical kinetics, and crossover issues, which can be addressed by the proper incorporation of suitable additives or complexing agents to improve membrane conductivity. The above operations could result in the commercialisation of polysulfide-iodide RFB.

5. Acknowledgement

M. U. acknowledges the Research Fund (Project number: 24KUJoint10) support received from Daegu Gyeongbuk Institute of Science and Technology (DGIST), Korea, through the International Joint Research Program. M.A., and M. U. also acknowledges Amrita Vishwa Vidyapeetham for the financial support received through the AMRITA Seed Grant (Proposal ID: ASG2022069).

6. References

1. Naval N, Yusta JM, Sánchez R, Sebastián F. Optimal scheduling and management of pumped hydro storage integrated with grid-connected renewable power plants. J Energy Storage. 2023; 73:108993. https://doi.org/10.1016/j.est.2023.108993
2. Bamisile O, Zheng Z, Adun H, Cai D, Ting N, Huang Q. Development and prospect of flywheel energy storage technology: A citespace-based visual analysis. Energy Rep. 2023; 9:494-505. https://doi.org/10.1016/j.egyr.2023.05.147
3. Zhang X, Gao Z, Zhou B, Guo H, Xu Y, Ding Y, *et al*. Advanced compressed air energy storage systems: Fundamentals and applications. Engineering. 2024; 34, 246–269. https://doi.org/10.1016/j.eng.2023.12.008
4. Kavoosi A, Hagh MT. Solid gravity energy storage: Pioneering energy storage solution–A review. J Energy Storage. 2025; 113, 115691. https://doi.org/10.1016/j.est.2025.115691
5. Rosa MD, Meleddu M, Pulina M. Contextual drivers of energy demand and supply from renewable sources. Heliyon. 2024; 10, e39727. https://doi.org/10.1016/j.heliyon.2024.e39727 PMid:39678256 PMCid:PMC11639454
6. Selvaraj M, Balamoorthy E, Manivasagam TG. Biomass derived nitrogen-doped activated carbon and novel biocompatible gel electrolytes for solid-state supercapacitor applications. J Energy Storage. 2023; 72, 108543. https://doi.org/10.1016/j.est.2023.108543
7. Baji DS, Kannan S, Madambikattil PB, Thirumurugan A, Sharma MK, Pai RK, *et al*. Overarching advancements in building practical Li-S batteries: A holistic review. J Energy Storage. 2024; 100, 113412. https://doi.org/10.1016/j.est.2024.113412
8. Arya TV, Aparnasree M, Ulaganathan M. MoO_3 modified graphite felt electrode for Zn-Fe redox flow cell applications. J Power Sources. 2025; 645, 237112. https://doi.org/10.1016/j.jpowsour.2025.237112

9. Sharmoukh W. Redox flow batteries as energy storage systems: Materials, viability, and industrial applications. RSC Adv. 2025; 15, 10106-10143. https://doi.org/10.1039/D5RA00296F PMid:40182497 PMCid:PMC11966388
10. Ulaganathan M. Zinc-iron (Zn-Fe) redox flow battery single to stack cells: A futuristics solution for high energy storage off-grid applications. Energy Adv. 2024; 3, 2861-2876. https://doi.org/10.1039/D4YA00358F
11. Niu Y, Gao Q, Zhao R, Liu Z, Zhou R, Yuan S, *et al*. A high current density and long cycle life iron chromium redox flow battery electrolyte. Green Chem Eng. 2024; 7(1), 61-69. https://doi.org/10.1016/j.gce.2024.09.007
12. Skyllas-Kazacos M, Kazacos G, Poon G, Verseema H. Recent advances with UNSW vanadium-based redox flow batteries. Int J Energy Res. 2009; 34, 182-189. https://doi.org/10.1002/er.1658
13. Gouveia J, Mendes A, Monteiro R, Mata TM, Caetano NS, Martins AA. Life cycle assessment of a vanadium flow battery. Energy Rep. 2020; 6, 95-101. https://doi.org/10.1016/j.egyr.2019.08.025
14. Monteiro R, Leirós J, Boaventura M, Mendes A. Insights into all-vanadium redox flow battery: A case study on components and operational conditions. Electrochimica Acta. 2018; 267, 80-93. https://doi.org/10.1016/j.electacta.2018.02.054
15. Xu Z, Fan Q, Li Y, Wang J, Lund PD. Review of zinc dendrite formation in zinc bromine redox flow battery. Renew Sustain Energy Rev. 2020; 127, 109838. https://doi.org/10.1016/j.rser.2020.109838
16. Zhang S, Gao S, Zhang Y, Song Y, Gentle IR, Wang L, *et al*. All-soluble all-iron aqueous redox flow batteries: Towards sustainable energy storage. Energy Storage Mat. 2025; 75, 104004. https://doi.org/10.1016/j.ensm.2025.104004
17. Lu G, Wang Z, Zhang S, Ding J, Luo J, Liu X. Cathode materials for halide-based aqueous redox flow batteries: Recent progress and future perspectives. Nanoscale. 2023; 15(9), 4250-60. https://doi.org/10.1039/D2NR07291B
18. Sun C, Zhang H. Review of the development of first-generation redox flow batteries: Iron- chromium system. ChemSusChem. 2022; 15(1), e202101798. https://doi.org/10.1002/cssc.202101798
19. Tam V, Savinell R, Wainright J. Controlling current distribution in slurry electrodes for all-iron redox flow batteries. J Electrochem Soc. 2025 Jul 1; 172(7), 070503. https://doi.org/10.1149/1945-7111/ade745
20. Li J, Xu Z, Wu M. Halogen enabled aqueous flow cells for large-scale energy storage: Current status and perspectives. J Power Sources. 2023; 581, 233477. https://doi.org/10.1016/j.jpowsour.2023.233477
21. Olabi AG, Allam MA, Abdelkareem MA, Deepa TD, Alami AH, Abbas Q, *et al*. Redox flow batteries: Recent development in main components, emerging technologies, diagnostic techniques, large-scale applications, and challenges and barriers. Batteries. 2023; 9(8), 409. https://doi.org/10.3390/batteries9080409
22. Li L, Zhang X, Lu Y, Chen X, Cheng H, Lu Y. Recent advances and future perspectives of membranes in iron-based aqueous redox flow batteries. Energy Mater Adv. 2025; 5, 0118. https://doi.org/10.34133/energymatadv.0118
23. Tian W, Du H, Wang J, Weigand JJ, Qi J, Wang S, *et al*. A review of electrolyte additives in vanadium redox flow batteries. Materials. 2023; 16(13):4582. https://doi.org/10.3390/ma16134582
24. Sharmoukh W. Redox flow batteries as energy storage systems: Materials, viability, and industrial applications. RSC Adv. 2025; 15(13):10106-10143. https://doi.org/10.1039/D5RA00296F
25. Noack J, Skyllas- Kazacos M, Thaller L, Tomazic G, Bjorn Jonshagen, Morrissey P. History of flow batteries. 2023; 29-52. https://doi.org/10.1002/9783527832767.ch2
26. Wang S, Xu Z, Wu X, Zhao H, Zhao J, Liu J, *et al*. Excellent stability and electrochemical performance of the electrolyte with indium ion for iron–chromium flow battery. Electrochim Acta. 2021; 368:137524. https://doi.org/10.1016/j.electacta.2020.137524
27. K. Gong et al., "All-Soluble All-Iron Aqueous Redox-Flow Battery," ACS Energy Lett, 2016; 1(1), 89–93, https://doi.org/10.1021/acsenergylett.6b00049.
28. Li Z, Zhang Y, Zheng S, Tan H, Deng Y, Fan B. Multi-ligand chromium ion complexes for near-neutral iron–chromium complex high-voltage flow batteries. Chem Eng J. 2025; 516:164200. https://doi.org/10.1016/j.cej.2025.164200
29. Bae CH, Roberts EPL, Dryfe RAW. Chromium redox couples for application to redox flow batteries. Electrochim Acta. 2002; 48(3):279-287. https://doi.org/10.1016/S0013-4686(02)00649-7
30. Pecsok RL, Shields LD, Schaefer WP. Complexes of Chromium(II) and (III) with ethylenediaminetetraacetic acid. Inorg Chem. 1964; 3(1):114-116. https://doi.org/10.1021/ic50011a024
31. Walsh JH, Earley JE. Reduction potentials of some Chromium(III) complexes. Inorg Chem. 1964; 3(3):343-347. https://doi.org/10.1021/ic50013a009
32. Bae C, Roberts EPL, Chakrabarti MH, Saleem M. All-Chromium Redox Flow Battery for Renewable Energy Storage. Int J Green Energy. 2011; 8(2):248-264. https://doi.org/10.1080/15435075.2010.549598
33. He C, Zhang Y, Zhang S, Peng X, Noack J, Skyllas-Kazacos M, *et al.* Aqueous iron-based redox flow batteries for large-scale energy storage. Natl Sci Rev. 2025; 12(7). https://doi.org/10.1093/nsr/nwaf218
34. R. F. Savinell and J. S. Wainright, "Iron Flow Battery with Slurry Electrode for Large Scale Energy Storage: Scale-Up, Intellectual Property, and Commercialization Challenges,"

Electrochem Soc Interface, 2023, 32(3), 61. https://doi.org/10.1149/2.F08233IF.
35. Hawthorne KL, Petek TJ, Miller MA, Wainright JS, Savinell RF. An investigation into factors affecting the iron plating reaction for an all-iron flow battery. J Electrochem Soc, 162(1):A108. https://doi.org/10.1149/2.0591501jes
36. Selverston S, Nagelli E, Wainright JS, Savinell RF. All-iron hybrid flow batteries with in-tank rebalancing. J Electrochem Soc. 2019; 166(10):A1725. https://doi.org/10.1149/2.0281910jes
37. Yu S, Yue X, Holoubek J, Xing X, Pan E, Pascal T, *et al*. A low-cost sulfate-based all iron redox flow battery. J Power Sources. 2021; 513:230457. https://doi.org/10.1016/j.jpowsour.2021.230457
38. Zhang S, Guo W, Yang F, Zheng P, Qiao R, Li Z. Recent progress in polysulfide redox-flow batteries. Batter Supercaps. 2019; 2(7):627-637. https://doi.org/10.1002/batt.201900056
39. Yang X, Nian Q, Wang Y, Hong H, Wei Z, Hou Y, *et al*. Advancements for aqueous polysulfide-based flow batteries: Development and challenge. EES Batteries. 2025; 1(5):1102-1113. https://doi.org/10.1039/D5EB00107B
40. Li Z, Weng G, Zou Q, Cong G, Lu YC. A high-energy and low-cost polysulfide/iodide redox flow battery. Nano Energy. 2016; 30:283-292. https://doi.org/10.1016/j.nanoen.2016.09.043
41. Li Z, Lu YC. Polysulfide-based redox flow batteries with long life and low levelized cost enabled by charge-reinforced ion-selective membranes. Nature Energy. 2021; 6(5):517-528. https://doi.org/10.1038/s41560-021-00804-x
42. Darling RM, Gallagher KG, Kowalski JA, Ha S, Brushett FR. Pathways to low-cost electrochemical energy storage: A comparison of aqueous and nonaqueous flow batteries. Energy Environ Sci. 2014; 7(11):3459-3477. https://doi.org/10.1039/C4EE02158D
43. A. Ahmad et al., "Optimized and cost-effective elemental-sulfur sodium polysulfide/sodium bromide aqueous electrolytes for redox flow batteries," J Power Sources, 2024, 614, https://doi.org/10.1016/j.jpowsour.2024.235013
44. Khan SA. UV-ATR spectroscopy study of the speciation in aqueous polysulfide electrolyte solutions. Int J Electrochem Sci. 2012; 7(1):561-568. https://doi.org/10.1016/S1452-3981(23)13359-1
45. Khan SA, Hughes RW, Reynolds PA. Raman spectroscopic determination of oxoanions in aqueous polysulfide electrolyte solutions. Vib Spectrosc. 2011; 56(2):241-244. https://doi.org/10.1016/j.vibspec.2011.03.001
46. Gross MM, Manthiram A. Long-life polysulfide–polyhalide batteries with a mediator-ion solid electrolyte. ACS Appl Energy Mater. 2019; 2(5):3445-3451. https://doi.org/10.1021/acsaem.9b00253
47. Zhou H, Zhang H, Zhao P, Yi B. A comparative study of carbon felt and activated carbon based electrodes for sodium polysulfide/bromine redox flow battery. Electrochima Acta. 2006; 51(28):6304-6312. https://doi.org/10.1016/j.electacta.2006.03.106
48. Zhao P, Zhang H, Zhou H, Yi B. Nickel foam and carbon felt applications for sodium polysulfide/bromine redox flow battery electrodes. Electrochima Acta. 2005; 51(6):1091-1098. https://doi.org/10.1016/j.electacta.2005.06.008
49. R. Yeetsorn, S. Chitvuttichot, A. Tuantranont, T. Treeratanaphitak, and J. Gostick, "Development of 3D-printed electrodes using polyacrylonitrile/ graphene composites for application in polysulfide bromide flow battery," *Chemical Engineering and Processing - Process Intensification*, vol. 211, p. 110233, 2025. https://doi.org/10.1016/j.cep.2025.110233
50. Rahimi M, Dehkordi AM, Roberts EPL. Magnetic nanofluidic electrolyte for enhancing the performance of polysulfide/iodide redox flow batteries. Electrochim Acta. 2021; 369:137687. https://doi.org/10.1016/j.electacta.2020.137687
51. Wang W, Luo Q, Li B, Wei X, Li L, Yang Z. Recent progress in redox flow battery research and development. Adv Funct Mater. 2012; 23(8):970-986. https://doi.org/10.1002/adfm.201200694
52. Wang Z. et al., "Synergy of single atoms and sulfur vacancies for advanced polysulfide–iodide redox flow battery," Nat. Commun., 2025, 16(1), 2885, https://doi.org/10.1038/s41467-025-58273-9
53. Zai J, Zhu Y, He K, Iqbal A, Huang S, Chen Z, *et al*. Sandwiched Cu7S4@graphite felt electrode for high performance aqueous polysulfide/iodide redox flow batteries: Enhanced cycling stability and electrocatalytic dynamics of polysulfides. Mater Chem Phys. 2020; 250:123143. https://doi.org/10.1016/j.matchemphys.2020.123143
54. M. Rahimi, A. Molaei Dehkordi, H. Gharibi, and E. P. L. Roberts, "Novel Magnetic Flowable Electrode for Redox Flow Batteries: A Polysulfide/Iodide Case Study," Ind. Eng. Chem. Res., 2021; vol. 60(2), 824–841. https://doi.org/10.1021/acs.iecr.0c05768.
55. Shin M, Noh C, Chung Y, Kwon Y. All iron aqueous redox flow batteries using organometallic complexes consisting of iron and 3-[bis (2-hydroxyethyl)amino]-2-hydroxypropanesulfonic acid ligand and ferrocyanide as redox couple. Chem Eng J. 2020; 398:125631. https://doi.org/10.1016/j.cej.2020.125631
56. Zeng YK, Zhou XL, An L, Wei L, Zhao TS. A high-performance flow-field structured iron-chromium redox flow battery. J Power Sources. 2016; 324:738-744. https://doi.org/10.1016/j.jpowsour.2016.05.138